THE JOURNAL OF BIOLOGICAL CHEMISTRY VOL. 281, NO. 20, pp. 14350–14360, May 19, 2006

Methylation-independent Binding to Histone H3 and Cell Cycle-dependent Incorporation of HP1β into Heterochromatin*[S]◆

Received for publication, January 19, 2006, and in revised form, March 13, 2006 Published, JBC Papers in Press, March 18, 2006, DOI 10.1074/jbc.M600558200

George K. Dialynas[‡1,2], Dimitra Makatsori[‡1], Niki Kourmouli[§], Panayiotis A. Theodoropoulos[§], Kevin McLean[¶], Stefan Terjung[‖], Prim B. Singh[3], and Spyros D. Georgatos[‡4]**

*From the [‡]Stem Cell and Chromatin Group, Laboratory of Biology, The University of Ioannina, School of Medicine and Ioannina Biomedical Research Institute/Foundation for Research and Technology, 45 110 Ioannina, Greece, the [§]Department of Basic Sciences, University of Crete, School of Medicine, 95 110 Heraklion, Crete, Greece, the [¶]Functional Genomics Unit, Moredun Research Institute, EH26 0PZ Penicuik, Midlothian, Scotland, United Kingdom, the [‖]Advanced Light Microscopy Facility (ALMF), European Molecular Biology Laboratory, 69117 Heidelberg, Germany, and the **Nuclear Reprogramming Laboratory, Department of Gene Expression and Development, Roslin Institute, EH25 9PS Edinburgh, Scotland, United Kingdom*

We have examined HP1β-chromatin interactions in different molecular contexts *in vitro* and *in vivo*. Employing purified components we show that HP1β exhibits selective, stoichiometric, and salt-resistant binding to recombinant histone H3, associating primarily with the helical "histone fold" domain. Furthermore, using "bulk" nucleosomes released by MNase digestion, S-phase extracts, and fragments of peripheral heterochromatin, we demonstrate that HP1β associates more tightly with destabilized or disrupted nucleosomes (H3/H4 subcomplexes) than with intact particles. Western blotting and mass spectrometry data indicate that HP1β-selected H3/H4 particles and subparticles possess a complex pattern of post-translational modifications but are not particularly enriched in me_3K9-H3. Consistent with these results, mapping of HP1β and me_3K9-H3 sites *in vivo* reveals overlapping, yet spatially distinct patterns, while transient transfection assays with synchronized cells show that stable incorporation of HP1β-gfp into heterochromatin requires passage through the S-phase. The data amassed challenge the dogma that me_3K9H3 is necessary and sufficient for HP1 binding and unveil a new mode of HP1-chromatin interactions.

Histone modifications are thought to provide specific readouts that are selectively utilized in DNA transactions or chromatin state transitions (1). Given the multiplicity of modification sites and the diverse chemistries of post-translational modifications, the combinatorial repertoire of this putative "histone code" might have enormous dimensions; for instance, methylation of the five lysine residues that are located at the amino-terminal tail of histone H3 could yield alone over 15×10^3 distinct patterns, while "saturation marking" of all lysines, arginines, serines, and threonines that are found in the same region would result in $\sim 256 \times 10^6$ combinations. Clearly then, even if 1% of the predicted patterns were materialized *in vivo*, this voluminous "instruction manual" could not be functionally interpreted without the aid of specific de-coding factors. Consistent with this idea, recent studies have identified a set of chromatin-associated proteins that bind specifically modified histones and could, at least in theory, fulfil such a de-coding role. As it turns out, these "effector" molecules are often components of large enzymatic assemblies and possess specialized modules known as bromo-, tudor-, or chromodomains (2).

A classic example of a chromodomain-containing protein is HP1, a conserved constituent of eukaryotic cells, which, in metazoans, comprises three distinct variants: α, β, and γ (3). HP1α and HP1β are localized in compact heterochromatic regions, while HP1γ is more abundant in euchromatic territories (reviewed in Refs. 4 and 5). All HP1 variants have the same molecular architecture: they contain an amino-terminal chromodomain (CD),[5] an intervening region ("hinge") and a carboxyl-terminal chromoshadow domain (CSD). The CD is thought to be responsible for chromatin association, whereas the CSD represents a multipurpose binding platform for nuclear chaperones, remodeling factors, and histone-modifying enzymes (4, 5). Interaction sites are also accommodated in the hinge region, which, in addition, contains a functional nuclear localization signal (6).

Although the picture is rapidly changing (*e.g.* Ref. 7), it is still widely believed that HP1 targets transcriptionally inactive, constitutive heterochromatin by binding specifically to histone H3 that has been post-translationally modified (trimethylated) at lysine 9 (me_3K9-H3). This tenet is based on several observations: first, HP1α/HP1β largely co-localize with me_3K9-H3 (8, 9) and seem to accumulate in the neighborhood of silenced genes (7); in addition, these two variants are completely de-localized when the enzymes responsible for heterochromatin-specific Lys^9 trimethylation (SUV39H1/H2) are genetically ablated (8, 9); finally, me_3K9-H3 peptides and native H3 have been reported to bind HP1 *in vitro*, whereas unmodified peptides and recombinant H3 do not (10–13).

* This work was supported in part by PENED and EPAN grants from the General Secretariat of Research and Technology and by a Pythagoras-EPEAK grant from the Ministry of Education (Greece) (to S. D. G.), a core grant from the Biotechnology and Biological Science Research Council (United Kingdom) (to P. B. S.), and by a Royal Society (United Kingdom) exchange award (to P. B. S. and S. D. G.). The costs of publication of this article were defrayed in part by the payment of page charges. This article must therefore be hereby marked "*advertisement*" in accordance with 18 U.S.C. Section 1734 solely to indicate this fact.

This paper is dedicated to Giorgos Mathianakis.

◆ This article was selected as a Paper of the Week.

[S] The on-line version of this article (available at http://www.jbc.org) contains supplemental data and Figs. S1–S3.

[1] Both authors contributed equally to this work.

[2] Supported in part by an Ioannina Biomedical Research Institute/Foundation for Research and Technology-internal fellowship.

[3] Present address: Division of Tumor Biology, Dept. of Immunology and Cell Biology, Forschungszentrum Borstel, D-23845 Borstel, Germany.

[4] To whom correspondence should be addressed: Laboratory of Biology, University of Ioannina, School of Medicine, Dorouti, 45 110 Ioannina, Greece. Tel.: 302651097565; Fax: 302651097863; E-mail: sgeorgat@cc.uoi.gr.

[5] The abbreviations used are: CD, chromodomain; CSD, carboxyl-terminal chromoshadow domain; FRAP, fluorescence recovery after photobleaching; NG, Nuclear ghost; NGE, NG extract; DTT, dithiothreitol; PMSF, phenylmethylsulfonyl fluoride; BrdUrd, bromodeoxyuridine; GST, glutathione *S*-transferase; MALDI-TOF, matrix-assisted laser desorption ionization time-of-flight; LBR, lamin B receptor; D, diffuse; SP, speckled; me_1, methylated; me_3, trimethylated.

Despite the elegance and simplicity of this model, binary interactions between HP1 and me_3K9-H3 do not seem to account for the whole spectrum of HP1-heterochromatin associations that are observed *in vivo* (14). A survey of different organisms, cell types, and chromosomal preparations shows that the HP1 and me_3K9-H3 patterns are not exactly coincident (15, 16), while mapping of HP1 and me_3K9-H3 target loci in *Drosophila* reveals the existence of distinct binding sites (17–19). In line with these observations, HP1 seems to dissociate from heterochromatin when cellular components unrelated to Suvar3,9 (*e.g.*, the origin recognition complex protein ORC2 or RNA) are removed (20–24). Last, but not least, *in vitro* binding of HP1 to non-methylated histone H3 and naked DNA has been recently claimed (25–27), contradicting some of the previous observations.

Prompted by current controversies, we decided to study HP1-chromatin interactions at different levels of complexity. Purified histones were employed to examine the binding properties of HP1 independently of chromatin state and presence of auxiliary factors. Alternatively, "bulk" chromatin, released from nuclei by MNase digestion, was used to investigate the association of HP1 with native particles of different size and epigenetic status. Finally, chromatin fragments obtained from fractionated "nuclear ghost" and S-phase extracts were exploited to assess HP1 interactions with intact core particles and assembly/disassembly intermediates.

Aiming at specific, stoichiometric interactions, we adopted a "μg-scale" binding assay and analyzed HP1-associated histones by SDS-PAGE-Coomassie Blue staining and mass spectrometry, avoiding purposely the use of radiolabeled tracers (*in vitro* transcribed/translated material) and resorting to Western blotting only when we wanted to "diagnose" epigenetic modifications. These *in vitro* studies were done in parallel with *in vivo* experiments, employing transient transfection assays, double-immunolabeling in combination with confocal microscopy, and fluorescence recovery after photobleaching (FRAP). The data reveal a new mechanism of HP1 binding to histone H3 and strongly suggest that stable incorporation of this protein in chromatin territories occurs after passage through the S-phase.

MATERIALS AND METHODS

Cells and Antibodies—Turkey erythrocytes were obtained from whole blood. HeLa, MCF-7, NRK, and MDCK2 cells were cultured according to standard procedures. Anti-acetylated Lys^{14}-H3 and anti-SNF2 polyclonal antibodies were purchased from Upstate Biotechnology, Lake Placid, NY. The characterization of anti-me_3K9-H3 and anti-me_3K20-H4 antibodies has been described (15, 28). CREST human autoimmune serum was kindly provided by W. C. Earnshaw (University of Edinburgh, Edinburgh, UK).

Cell Cycle Arrest—Early S-phase cells were obtained by treatment with 5 mM hydroxyurea for 24 h. Alternatively, we used 3 μg/ml aphidicolin for 24 h, 0.5 mM mimosine for 24 h, or a double thymidine block (19 h in 2 mM thymidine, 9-h release, 16 h in 2 mM thymidine).

Cell Fractionation and Preparation of Nuclear Extracts—Nuclear ghosts (NGs) were prepared from turkey erythrocyte nuclei, as specified (29). Briefly, after three rounds of DNase I digestion (80 μg/ml in 10 mM NaPO4, 2 mM $MgCl_2$, 10% sucrose, 1 mM DTT, 1 mM PMSF/protease inhibitors, 15 min, at room temperature, with 200 μg/ml RNase A included in the last digestion step), the resulting NGs were washed in buffer I (150 mM NaCl, 20 mM Tris-HCl pH 7.5, 250 mM sucrose, 2 mM $MgCl_2$, 0.1 mM EGTA, 1 mM DTT, 1 mM PMSF), sonicated to induce vesiculation, and stored at −80 °C. Extracts were prepared by thorough resuspension of sonicated NGs in 300–600 mM NaCl, 20 mM Tris-HCl, pH 7.5, 250 mM sucrose, 2 mM $MgCl_2$, 0.1 mM EGTA, 1 mM DTT, 1 mM PMSF, protease inhibitors. After ultracentrifugation (200–350,000 × *g*, 30 min, 4 °C), the soluble extracts were collected and either used immediately or further fractionated in 10–30% sucrose density gradients (100,000 × *g*, 4 °C, 18 h). For preparation of S-phase extracts, HeLa cells were synchronized using double thymidine block, collected by trypsinization, washed three times with isotonic buffer (150 mM NaCl, 20 mM Hepes, pH 7.4, 2 mM $MgCl_2$, 1 mM PMSF), and resuspended in buffer A (150 mM NaCl, 20 mM Hepes, pH 7.4, 2 mM $MgCl_2$, 1 mM $CaCl_2$, 0.25% Triton X-100, 250 mM sucrose, 1 mM DTT, 1 mM PMSF, 2 μg/ml protease inhibitors). Cells were treated with MNase (5 units/10^6 cells or 1,500 units/ml of pellet) for 10 min at 37 °C, incubated on ice for 10 min after addition of 2 mM $CaCl_2$, and centrifuged at 13,000 × *g*, for 10 min at 4 °C. The supernatant (F1) was collected, and the salt concentration was adjusted to 300 or 600 mM. The pellet was resuspended in ice-cold 2 mM EDTA, pH 7.5, and centrifuged as above. The supernatant was collected and the salt adjusted to 300 or 600 mM (F2). The pellet was further extracted with 300 mM salt buffer (300 mM NaCl, 20 mM Tris-HCl, pH 7.5, 250 mM sucrose, 2 mM $MgCl_2$, 0.1 mM EGTA, 1 mM DTT, 1 mM PMSF, protease inhibitors) and 1% Triton X-100, centrifuged at 100,000 × *g*, for 30 min at 4 °C, and the supernatant (F3) collected. Equivalent amounts of fractions F1, F2, and F3 were used for pulldown assays.

Microscopy—For light microscopy, samples were fixed with 1–4% formaldehyde in phosphate-buffered saline, permeabilized with 0.2% Triton X-100, and blocked with 0.5% fish skin gelatin. DNA staining (propidium iodide) and probing with the relevant primary and secondary antibodies was performed according to Maison *et al.* (30). BrdUrd staining was done as specified by manufacturer (Roche Diagnostics GmbH, Penzberg, Germany).

Pulldown Assays—GST fusion proteins (HP1α, HP1β, and HP1γ or GST alone; ~15–30 μg) were incubated first for 30 min at room temperature with 30 μl of glutathione-agarose beads, "blocked" in 1% fish gelatin in assay buffer. After washing three times with the same medium, the beads were combined with nuclear extracts and further incubated for 1 h at room temperature. The beads were washed six times with buffer, before eluting the bound proteins with hot SDS-sample buffer.

Other Methods—MALDI-TOF mass spectrometry was performed at the Functional Genomics Unit of Moredun Research Institute, Edinburgh, UK. Protein bands were digested with R-specific protease. Δ*M* (difference between measured and calculated masses) was at the level of 1/10,000. Peak assignment was done either manually or using Applied Biosystems programs. Trypsin digestion experiments were performed using 100 μl of trypsin cross-linked to agarose beads (19.5 units/ml) incubated with the corresponding protein (recombinant H3) for 0, 2, and 10 min at 4 °C. The reaction was terminated by addition of trypsin and protease inhibitors. The digests were ultracentrifuged at 200–350,000 × *g* (30 min, 4 °C) and then used for pulldown experiments. SDS-PAGE, Western blotting, column chromatography, and microinjection were practiced according to established procedures. Morphometric analysis and assessment of co-localization of different markers were performed using stacks of confocal images digitally processed and analyzed by Image J.

RESULTS

HP1 Binding to Purified Histones and Histone Peptides—To examine the binding preference of HP1, we first assayed total histones extracted from avian erythrocyte nuclei by 0.1 M H_2SO_4. As shown in Fig. 1*A*, HP1β-GST precipitated almost exclusively histone H3. Consistent with this, HP1β bound stoichiometrically to recombinant histone H3 but

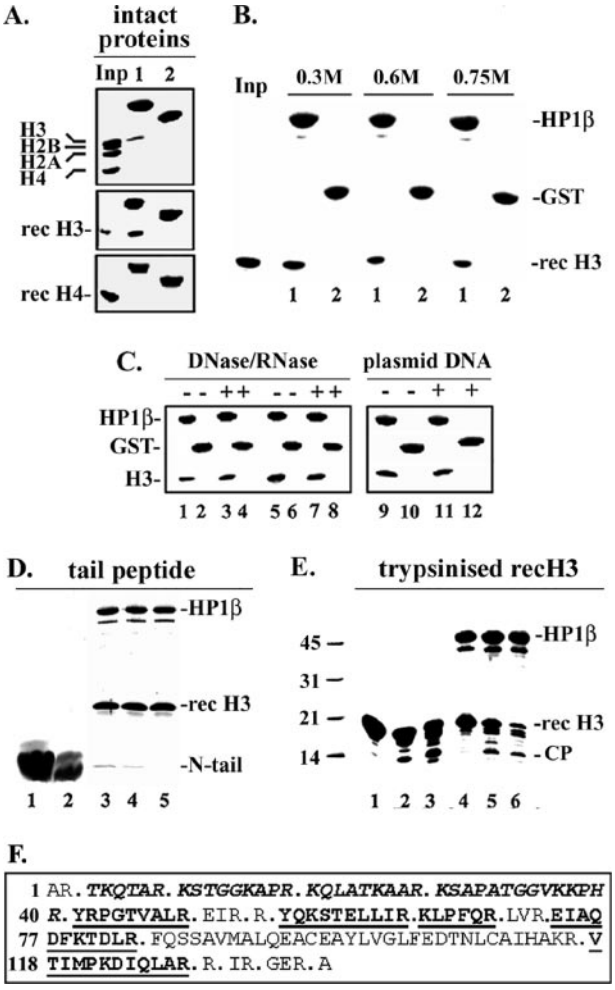

FIGURE 1. **HP1 binding to isolated histones and histone peptides.** *A*, material precipitated by HP1β (*lanes 1*), or GST (*lanes 2*), upon co-incubation with a mixture of erythrocyte histones, recombinant H3 (*rec H3*), or recombinant H4 (*rec H4*). (*Inp*) is 50% of the input. *B*, recombinant H3 precipitated by HP1β (*lanes 1*), or GST (*lanes 2*), at 0.3, 0.6, and 0.75 M salt. *Inp* is 50% of the input. *C*, histone H3 precipitated by HP1β (*odd-numbered lanes*) or GST (*even-numbered lanes*) after treatment with DNase I/RNase A and in the presence of plasmid DNA, as indicated. Both recombinant (*lanes 1–4* and *9* and *10*) and native (*lanes 5–8* and *11* and *12*) histones were used. *D*, binding of recombinant H3 to HP1β in the presence of a 200-fold excess of the unmodified tail peptide (*lane 3*), the me_3K9-modified peptide (*lane 4*), or buffer (*lane 5*). *Lanes 1* and *2* show electrophoretic profiles of the unmodified and the modified H3 peptide, respectively. HP1β, recombinant H3, and co-precipitating peptides (*N-tail*) are indicated. *E*, digestion of recombinant H3 with trypsin beads for 0 min (*lane 1*), 2 min (*lane 2*), and 10 min (*lane 3*). *Lanes 4–6*, material precipitated from each of these digests by HP1β. A peptide corresponding to the "fold" domain of histone H3 (*CP*) and the intact protein are indicated. Lane on the left corresponds to molecular mass markers (in kDa). *F*, sequences of the CP peptide, as detected by mass spectrometry. Stretches that are expected to yield distinct peaks (see also Fig. 6) are in *bold*, whereas products that were either too small or too large for analysis by MALDI-TOF are in *regular letters*. Detected peptides are *underlined*. The protein has been cleaved with R-specific protease and the data analyzed statistically by Mascot Search.

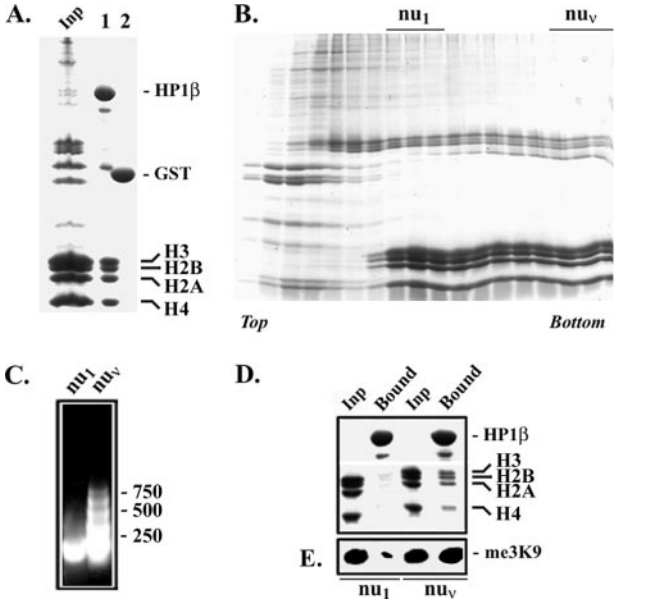

FIGURE 2. **HP1 binding to mononucleosomes and oligonucleosomes.** *A*, HP1 binding to bulk chromatin, released from nuclei after MNase digestion. *Lane 1*, material precipitated by HP1β at 0.3 M salt; *lane 2*, corresponding GST control. *Inp* indicates a sample of the input material (20%). *B*, fractionation of the MNase digest by centrifugation in a 10–30% sucrose gradient. Fractions corresponding to mononucleosomes and oligonucleosomes are designated (nu_1) and (nu_v), respectively. *C*, DNA profile of fractions (nu_1) and (nu_v). Sizes (in bp) are indicated on the *right*. *D*, pulldown assay with selected gradient fractions. In each case *Inp* indicates the input material (20%) and *Bound* the HP1β precipitate. *E*, Western blot with anti-me_3K9 antibodies corresponding to the samples shown in *D*.

failed to associate with recombinant histone H4 (Fig. 1*A*, *rec H4* and *rec H3*). Binding to recombinant H3 was tight and easily detectable even at 0.75 M salt (Fig. 1*B*). Since no significant differences were seen when HP1β or histones were treated with DNase I/RNase A or when stoichiometric amounts of plasmid DNA were included in the assay (Fig. 1*C*), nonspecific interactions mediated by nucleic acid contaminants could be safely ruled out.

As shown in Fig. 1*D*, "tail" peptides that represented either the non-modified or the me_3K9-modified NH_2-terminal region of H3 exhibited marginal binding to HP1β at 0.3 M salt and did not compete with the full-length protein, even at a 200 molar excess. However, when H3 was digested with trypsin, a proteolytic product with an apparent M_r of 12,000 was detected in the HP1β precipitate (Fig. 1*E*, *CP*). On the basis of previously published studies (31–33) and results shown in Fig. 1*F*, this fragment can be assigned to the stretch extending between amino acids 40–129, *i.e.* the so-called "histone fold" domain. Thus, at least under *in vitro* conditions, HP1β has the capacity to bind histone H3 independently of post-translational modifications, associating primarily with the central, helical part of the molecule.

HP1 Interactions with Fragments of Native Chromatin—To study HP1 interactions with bulk chromatin, we used as a substrate material released from G_0 nuclei after MNase digestion. As shown in Fig. 2*A*, when the whole digest was used as input, HP1β precipitated stoichiometric amounts of histone proteins. However, when chromatin was fractionated on sucrose density gradients (Fig. 2, *B* and *C*) and individual fractions assayed, we noticed that HP1β bound almost exclusively to oligonucleosomal arrays (nu_v) and did not interact significantly with mononucleosomes (nu_1) (Fig. 2*D*). The higher propensity of HP1β to bind oligonucleosomes was not due to "enrichment" in me_3K9 histone H3, as documented in the Western blot shown in Fig. 2*E*. Furthermore, no differences were seen when the experiments were done at 0.3 and 0.6 M salt (data not shown), a point that will be taken up next.

Continuing these studies, we then examined S-phase chromatin, which is expected to contain a variety of nucleosome assembly/disassembly intermediates (34, 35). Cultured cells were arrested at G_1/S with a double thymidine block and then released for 7 h to allow progression to mid-S (Fig. 3*A*, *inset*). A "soluble" chromatin fraction (F1) was collected after lysis with Triton X-100 and "nicking" with MNase (mild nuclease digestion was deemed necessary to release detached particles trapped in tangles of non-replicating chromatin). Larger fragments of euchromatin (F2) and heterochromatin (F3) were subsequently extracted from the Triton-insoluble residue by serial washing with 2 mM EDTA and 0.3 M NaCl (see diagram in Fig. 3*A*).

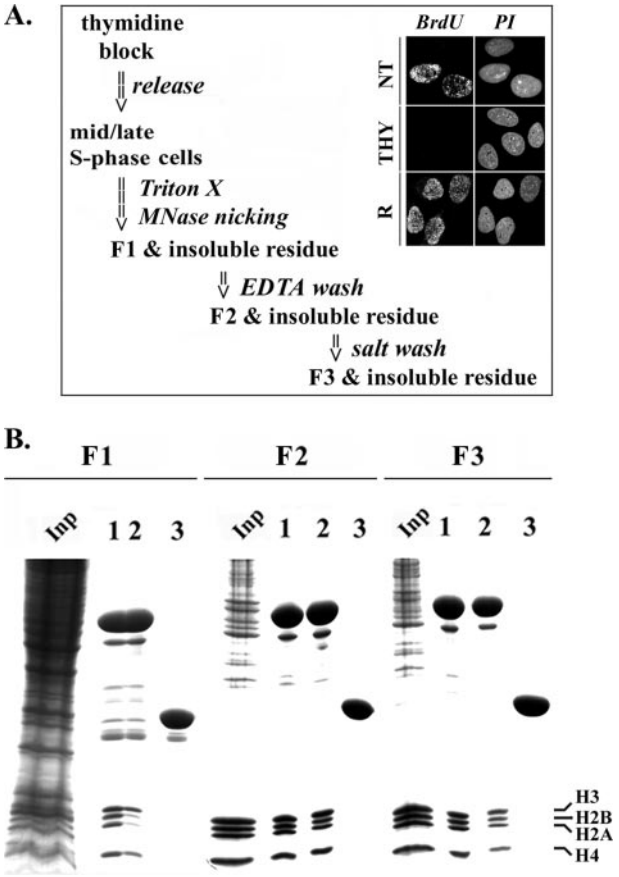

FIGURE 3. **HP1 binding to fractions of S-phase chromatin.** *A*, diagram showing the scheme used to fractionate S-phase chromatin. The *inset* shows HeLa cells stained with BrdUrd (*BrdU*) and propidium iodide (*PI*) before synchronization (*NT*), after thymidine block (*THY*), and after release for 7 h in normal medium (*R*). *B*, binding of HP1β to nucleosomal particles extracted from S-phase cells. *Lanes 1* and *2*, material associated with HP1β at 0.3 and 0.6 M salt, respectively; *lanes 3*, GST controls (at 0.3 M salt). *Inp* indicates 20% of the material added in each assay. *F1*, *F2*, and *F3* correspond to chromatin-solubilized sequentially by Triton X-100, EDTA and 0.3 M salt.

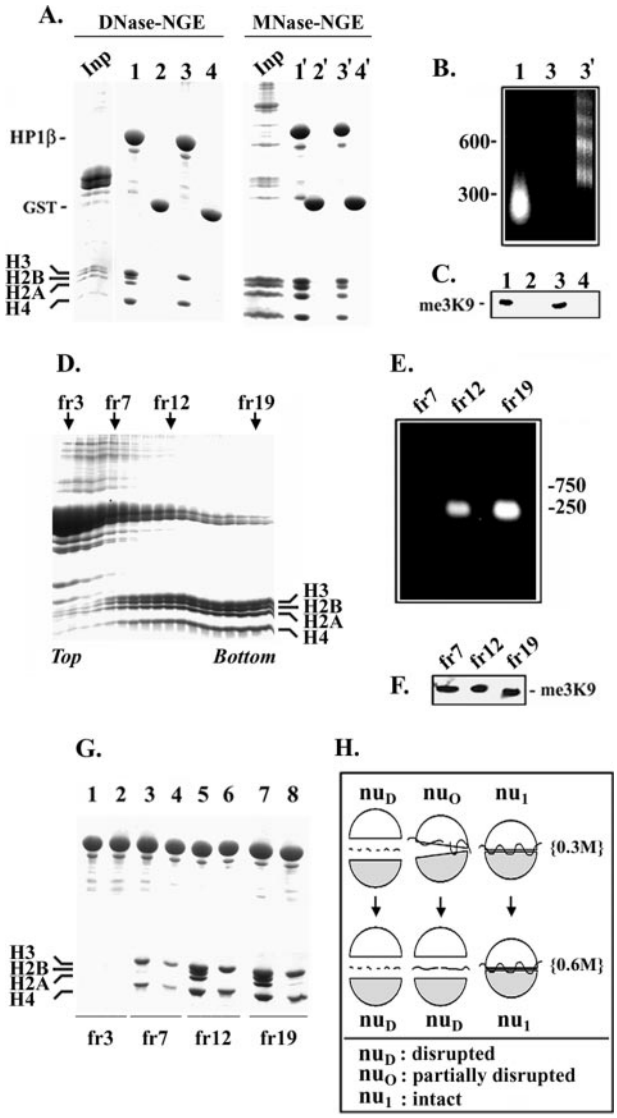

FIGURE 4. **HP1 binding to disrupted nucleosomes.** *A*, HP1 binding to fragments of peripheral heterochromatin extracted from nuclease-digested nuclei (nuclear ghosts). *Lanes 1* and *1′* and *3* and *3′*, material precipitated by HP1β at 0.3 and 0.6 M NaCl, respectively; *lanes 2* and 2′ and 4 and 4′, corresponding GST controls. *Inp* indicates a sample (20%) of the input extract. Group *DNase-NGE* corresponds to extracts of DNase I-digested nuclei, whereas *MNase-NGE* to extracts of MNase-digested nuclei (for more details see "Results.") *B*, DNA co-precipitating with HP1β and histones in the experiment presented above. Lanes are exactly as specified for *A*. Markers (in bp) are shown on the *left*. *C*, Western blotting using anti-me_3K9 antibodies. Lanes are exactly as indicated for *A*. *D*, fractionation of the nuclear ghost extract (*DNase-NGE*) in a 10–30% sucrose gradient. Fractions used in subsequent experiments are indicated by *arrows*. *E* and *F*, DNA profile and Western blot of the fractions indicated in *D*. Markers (in bp) are shown on the *right*. *G*, pulldown assay with the fractions shown above. *Odd-numbered lanes* correspond to samples assayed at 0.3 M, while *even-numbered lanes* correspond to samples assayed at 0.6 M salt. *H*, schematic describing in hypothetical terms the particle types present in nuclear ghost extracts. Nucleosomal DNA is represented by *broken* or *wavy lines*; H2A-H2B and H3-H4 subcomplexes are shown as *semicircles*. For further details see "Results."

When the F1 fraction was used as input and the assay performed at 0.3 M salt, HP1β precipitated apparently intact histone octamers (Fig. 3*B*, *F1*, *lane 1*). However, when the same experiment was done at 0.6 M salt, the HP1β precipitate contained predominantly H3/H4 (Fig. 3*B*, *F1*, *lane 2*), suggesting that Triton-soluble particles are labile and probably represent non yet stabilized (nascent) or de-stabilized nucleosomes (for relevant data, see Ref. 36). Supporting this interpretation, no salt-dependent effects were observed with fractions F2 and F3 (Fig. 3*B*, *F2* and *F3*, compare *lanes 1* and *2*), which are known to contain stable, detergent-insoluble chromatin pieces (*i.e.* polynucleosomes).

HP1 Interactions with Intact Particles and Subparticles Derived from Heterochromatin—In combination, the observations presented in Figs. 2 and 3 indicated that HP1β does not bind to intact mononucleosomes released from G_0 chromatin but does bind oligonucleosomes and "salt-labile", detergent-soluble fragments extracted from S-phase chromatin. Since these preparations represented bulk chromatin, not particularly enriched in any single histone modification, we wondered what would happen if the input contained native particles that are specifically modified in Lys^9-H3. To answer this question, we used fractions derived from peripheral heterochromatin. In a previous study we have shown that mononucleosomes highly enriched in me_3K9 and depleted of me_3K4 can be obtained in high yield by 0.3 M NaCl extraction of nuclear ghosts, *i.e.* G_0 nuclei that have been extensively digested with DNase I and sonicated, to release pieces of heterochromatin firmly attaching to the nuclear envelope (for procedural details and mass spectrometry data, see Ref. 29). When such extracts (DNase-NGEs) were co-incubated with HP1β under different ionic conditions, we observed an interesting and highly reproducible pattern. At 0.3 M salt, HP1β precipitated the four core histones, *en bloc* with fragments of DNA containing 100–250 bp (Fig. 4, *A* and *B*, *lanes 1*). However, upon closer inspection, one could easily see that the ratio of the core histones in the HP1β precipitate was slightly "skewed" in favor of H3/H4. This "preference" became pronounced when the assay was executed in 0.6 M salt, at which point

HP1β brought down only H3/H4 subparticles that were essentially DNA-free (Fig. 4, *A* and *B*, *lanes 3*).

The characteristic pattern was not observed when the input material contained larger particles. Peripheral heterochromatin extracts containing oligonucleosomes rather than mononucleosomes could be easily prepared by digesting the nuclei with MNase instead of DNase I, taking advantage of the fact that the former is much less aggressive a nuclease than the latter (37, 38). When these extracts (MNase-NGEs) were tested at different salt conditions, HP1β precipitated equimolar amounts of the four core histones and DNA fragments consisting of 150-mer even at 0.6 M salt. This experiment proves that histone octamers do not disassemble by a mere salt "jump" from 0.3 M to 0.6 M NaCl, unless nucleosomal DNA has been extensively cut (for further details see below). This is not inconsistent with the current literature: the breakpoint at which H2A/H2B separate from H3/H4 and DNA unwraps from the particle lies somewhere between 0.5 and 1 M NaCl (11, 39–42); however, the exact "transition zone" seems to depend critically on Mg^{2+} and nucleosome concentration (11, 39–42).

Since histone H3 precipitated from DNase-NGEs at 0.3 and 0.6 M salt did not differ with regards to Lys^9 trimethylation (Fig. 4*C*), the data presented in Fig. 4*A* could be interpreted to mean that under stringent conditions HP1β exhibits preferential binding to H3/H4 subparticles.

That such disrupted nucleosomes pre-existed in the input material and did not originate from salt-induced disassembly could be confirmed by separating DNase-NGEs on sucrose density gradients at 0.3 M NaCl (Fig. 4, *D–F*) and assaying different fractions at both 0.3 and 0.6 M salt. As shown in Fig. 4*G* (*lanes 3* and *4*), when low density material (*e.g. fr7*) was used as input, HP1β precipitated exclusively H3/H4 at both salt concentrations. However, when material collected from the middle/high density zone (*e.g. fr12-fr19*) was tested in the same way, the binding pattern was clearly salt-dependent and resembled that observed with the whole, non-fractionated DNase-NGEs (compare Fig. 4*G*, *lanes 5–8*, with Fig. 3*A*, *lanes 1–4*). Evidently, HP1β did not bind linker histones (Fig. 4*G*, *lanes 1* and *2*) that were abundantly present in the top fractions of the gradient (Fig. 4*D*).

The interpretation we offer to explain these results is presented in the cartoon of Fig. 4*H*. We argue that the low density fractions of the gradient shown in Fig. 4*D* contain predominantly disrupted particles (nu_D). These probably originate from nucleosomes whose DNA has been completely digested during chromatin preparation (removal of DNA is known to weaken H2A/H2B-H3/H4 interactions and favor particle dissociation; reviewed in Ref. 43). We further suggest that the middle/high density fractions are enriched in intact mononucleosomes (nu_1) and particles that lack various parts of nucleosomal DNA and are partially "open" (nu_O). Unlike nu_1, nu_O can bind HP1β at permissive conditions, similarly to nu_D and non-stabilized S-phase intermediates. "Skewing" in favor of H3/H4 is observed at 0.3 M salt (Fig. 4, *A* and *G*), because octameric units (nu_O), as well as half-particles consisting of H3/H4, are co-precipitated with HP1β. This becomes more pronounced when the salt is increased, as "unstable" nu_O split and are converted to nu_D. Since nu_1 contain intact nucleosomal DNA and are not salt-labile, only two particle species remain at 0.6 M NaCl: these that bind HP1β (nu_D) and those that do not (nu_1).

To directly examine whether disrupted particles were more apt to associate with HP1β than intact mononucleosomes, we took advantage of the fact that LBR, a chromatin-binding protein structurally unrelated to HP1, has a predilection for intact nucleosomes (Ref. 31; see Fig. S1 in supplemental data). Knowing that, we assessed binding using as input a preparation that contained both fully and partially assembled nucleosomes (44). Results presented in Fig. 5*A* make it clear that under the same (permissive) conditions, and at equivalent protein concentration LBR "collects" octameric particles, while HP1β selects predominantly H3/H4 complexes.

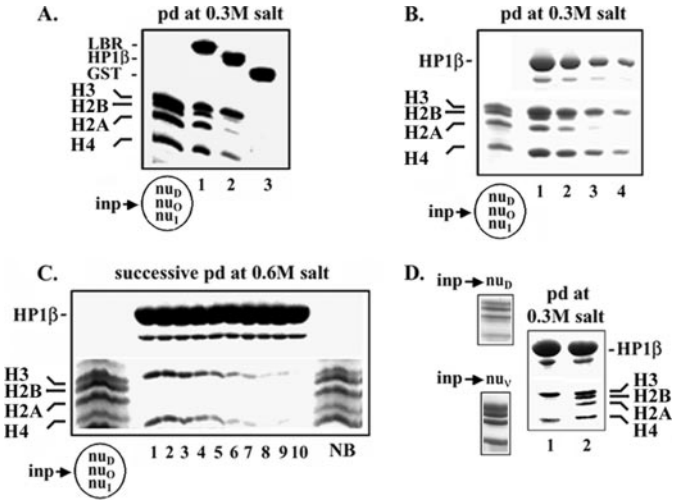

FIGURE 5. **Selective binding of HP1 to H3/H4 sub-particles.** *A*, particles "selected" by LBR (*lane 1*), HP1β (*lane 2*), and GST (*lane 3*) from a mixture of fully and partially assembled nucleosomes at 0.3 M salt. *Inp* represents 20% of the input. *B*, pulldown assays with varying amounts of HP1β (decreasing from *lane 1* to *lane 4*) at 0.3 M salt. *Inp* represents 20% of the input extract, which contains nu_1, nu_O, and nu_D. *C*, histones precipitated by recombinant HP1β in 10 consecutive pull downs at 0.6 M NaCl (*lanes 1–10*). Samples of the nuclear ghost extract (*Inp;* 20%) and the non-bound material (*NB;* 20% of total) are included. *D*, histones co-sedimenting with HP1β when the input (*Inp*, 20%) contained disrupted particles (nu_D, *lane 1*), or oligonucleosomes (nu_n, *lane 2*).

To further confirm these results, we performed pulldown assays under limiting conditions. As shown in Fig. 5*B*, H3/H4 complexes were preferentially precipitated at 0.3 M salt when the HP1β concentration in the reaction mixture was gradually decreased, suggesting selective binding to disrupted particles (nu_D). This could also be shown by successive pulldown assays at 0.6 M salt. In that case, HP1β was incubated with a fixed amount of DNase-NGEs, as described in the legend to Fig. 4*A*. After collecting the first precipitate, a new aliquot of the protein was added to the supernatant (non-bound fraction) and the procedure repeated nine more times. As illustrated in Fig. 5*C*, the extract was gradually depleted of H3/H4 subparticles, while a considerable amount of core histones, presumably representing intact mononucleosomes (nu_1), were left behind (compare lanes *Inp* and *NB*).

Finally, to eliminate factors that are peculiar to each chromatin isolation-fractionation technique we assessed side by side the binding properties of H3/H4 subparticles (*e.g.* nu_D, isolated as in Fig. 4*D*) with that of oligonucleosomes (*e.g.* nu_n, isolated as in Fig. 2*B*). Both species associated nearly stoichiometrically with HP1β (Fig. 5*D*).

Modification Patterns of HP1-associated Histone H3—To determine the modification "signatures" of HP1-associated histone H3, we isolated H3/H4 subparticles that bind to HP1β at 0.6 M salt (see Fig. 4*A*) and analyzed the samples by mass spectrometry. We also examined histone H3 precipitated in the context of octameric particles (*i.e.* at 0.3 M salt). In the latter case, all three HP1 variants (α, β, γ) were used in the pulldown experiments, to identify potential differences in binding preference.

Consistent with the biochemical data described above (Figs. 1–4), the modification patterns were identical in all histone H3 samples analyzed. As could be seen in Fig. 6*A*, methylation of K4 and double acetylation at Lys^{18}/Lys^{23} were not detected. However, affinity-selected H3 exhibited other interesting features, *e.g.* trimethylation in Lys^{79} and (mono)acetylation in Lys^{18}/Lys^{23}, which are, supposedly, "euchromatic" modifications. Among the species identified were also trimethylated Lys^{27}-H3 and methylated Lys^{36}-H3. Of these modifications, trimethylation of

A.

Peak (Da)	Peptide (res. no)	Potential modifications	Presence in HP1 precipitates	Modifiable lysines
704.4	3-8	nm	+	K4
718.4	3-8	me	-	K4
732.4	3-8	2Xme	-	K4
746.4	3-8	3Xme/ac	-	K4
901.5	9-17	nm	-	K9, K14
915.5	9-17	me	-	K9, K14
929.5	9-17	2Xme	+	K9, K14
943.5	9-17	3Xme/ac	+	K9, K14
971.5	9-17	5Xme/ac+2Xme	+	K9, K14
985.5	9-17	6Xme/ac+3Xme	+	K9, K14
986.6	18-26	nm	-	K18, K23
1028.6	18-26	ac	+	K18, K23
1070.6	18-26	2Xac	-	K18, K23
1433.8	27-40	nm	-	K27, K36
1447.8	27-40	me	-	K27, K36
1461.8	27-40	2Xme	+	K27, K36
1475.8	27-40	3Xme	+	K27, K36
1489.8	27-40	4Xme	+	K27, K36
1032.6	41-49	nm	+	K27, K36
1250.7	54-63	nm	+	K56
788.8	64-69	nm	+	K64
1335.6	78-83	nm	+	K79
1363.6	73-83	3Xme	+	K79
1384.8	117-128	nm	+	K122

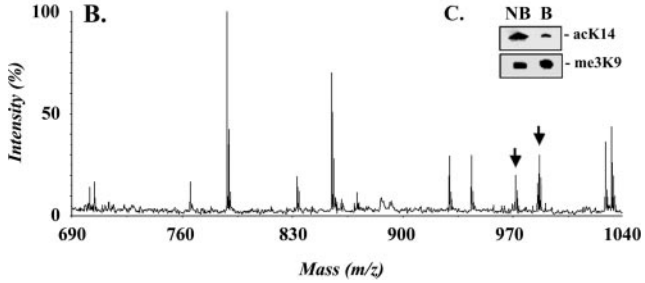

FIGURE 6. **Modification patterns of HP1-associated histone H3.** *A*, a list of the peaks detected by mass spectrometry in samples of histone H3 precipitated by HP1α, HP1β, and HP1γ. *nm*, non-modified residues; *me*, methylated residues; *ac*, acetylated residues. *B*, a segment of the mass spectrum depicting the most interesting peaks (those corresponding to 971.5 and 985.5 Da are indicated by *arrows*). *C*, Western blot of the HP1β-bound histones after probing with anti-me_3K9 and anti-acetyl Lys^{14}-H3 antibodies. Lanes correspond to the bound (*B*) and the non-bound (*NB*) fraction (100% of the material has been analyzed). The assays were performed at 0.6 M salt.

Lys^{27} has been associated with Polycomb-mediated gene silencing, while methylation of Lys^{36} is thought to provide a "transcription ON" signal (for a review, see Ref. 2).

The stretch of amino acids 9–17, which contains Lys^9 and Lys^{14}, was rather heavily modified. Since the mass difference corresponding to Lys trimethylation is very close to that of Lys acetylation, a peak at 971.5 Da could be assigned either to a (dimethylated + acetylated) or to a (dimethylated + trimethylated) peptide. Likewise, another peak at 985.5 Da could be attributed either to a twice trimethylated, or to a (trimethylated + acetylated) peptide (Fig. 6*B*). Since no histone methyltransferase specific for Lys^{14} has been described so far, while both me_3K9-H3 and acetylated Lys^{14}-H3 could be identified in HP1-precipitated H3 by Western blotting (Fig. 6*C*), we favor the latter interpretation. Be that as it may, the modification patterns detected were not diagnostic and did not conform to the formula "me_3K9/non-acetylated K14/me_1K27" that is thought to be necessary and sufficient for HP1 binding (11, 39–42).

Incorporation of HP1 into Chromatin under in Vivo Conditions—Our biochemical studies suggested strongly that HP1 proteins associate with different chromatin substrates in a manner that depends crucially on physical state. Since chromatin is a dynamic structure and undergoes multiple transitions during the cell cycle (43), we predicted that our *in vitro* observations likely had an *in vivo* correlate. To explore this idea, we employed a transient transfection system. Two different human cell lines (HeLa, MCF-7) and several methods of DNA uptake (microinjection, calcium phosphate treatment, or electroporation) were used in these experiments. Cells injected or porated with HP1β-gfp plasmids were examined at early (2–6 h) and late (12–24 h) time points, while calcium phosphate-transfected cells were visualized at 12, 24, and 48 h.

Irrespective of method, two distinct phenotypes were always detected among transfected cells: phenotype "SP" (after "speckled") included cells in which HP1β-gfp had accumulated at perinucleolar and peripheral heterochromatin; phenotype "D" (after "diffuse") represented another subpopulation in which the gfp-tagged protein did not follow the known stereotype and was diffusely distributed throughout the nucleoplasm, occasionally forming small granules (Fig. 7*A*). Interestingly, the relative proportions of SP and D cells changed with time in a rather orderly fashion (Fig. 7*B*): initially, accumulation of HP1β-gfp in heterochromatic areas was observed only in 30% of the cells; however, this proportion increased steadily, reaching a value of ~80% after 24 h. Similar results were obtained with non-human cells (*e.g.* canine MDCK2 cells, and rat NRK; data not shown).

The different patterns observed could be attributed to a variety of factors, including over-expression and, as a result, aberrant localization. For this reason, we first examined whether the distribution of HP1β-gfp correlated with fluorescence intensity. When the nuclei of numerous transfected cells were photographed and categorized, we could not detect an obvious connection between the overall fluorescence intensity and the specific HP1β-gfp pattern (Fig. 7*C*). However, it was noticeable that, on the average, SP cells had slightly larger nuclei than D cells (Fig. 7*D*). Taking this into account, we performed a morphometric study, recording precisely the ratio of fluorescence intensity/nuclear surface area (f_i/a) in 80 equatorial sections taken at the confocal microscope 6 h post-transfection. The results confirmed that overexpression does not account for the phenotypes observed: on the average, SP cells had only a marginal edge over D cells (differences in f_i/a ratio not exceeding 10%), while individual D and SP figures often exhibited exactly the same fluorescence intensity.

We could also confirm in a number of ways that assembly of HP1β-gfp in this transient transfection system was not "ectopic." First, HP1β-gfp and endogenous HP1β co-localized to more than 90% (Fig. 8*A*). Second, as expected from previous studies, HP1β-gfp foci fell well within heterochromatic regions (as defined by accumulation of me_3K9-H3 and me_3K20-H4) and outside euchromatic territories (as defined by SNF2 distribution) (Fig. 8, *B* and *C*). However, thorough inspection of transfected cells with confocal microscopy did reveal subtle features of the HP1 assemblies that were not immediately obvious during the initial screening of the specimens. For instance, whereas HP1β-gfp and endogenous HP1β were both present in heterochromatic foci, one could distinguish discrete subdomains, in which the relative proportion of the two proteins varied significantly (note "variegated" foci in the gallery of Fig. 8*A*). Moreover, it was clear in numerous (*xy*) and (*xz*) sections that HP1β-gfp and me_3K9-H3 do not exactly colocalize (Fig. 8*C*, *arrows*). Since HP1β-gfp was capable of targeting heterochromatic sites containing endogenous HP1β and exhibited normal dynamics (see below), steric effects due to the gfp moiety could be safely ruled out. Therefore, the spatially distinct patterns of HP1β-gfp and me_3K9-H3 fluorescence could mean that HP1β follows different assembly pathways, one of which is largely independent of Lys^9 trimethylation.

This idea was supported by other experiments. For instance, when human cells were transfected with two HP1β mutants (one possessing only the CD and the other containing the hinge plus the CSD), or a

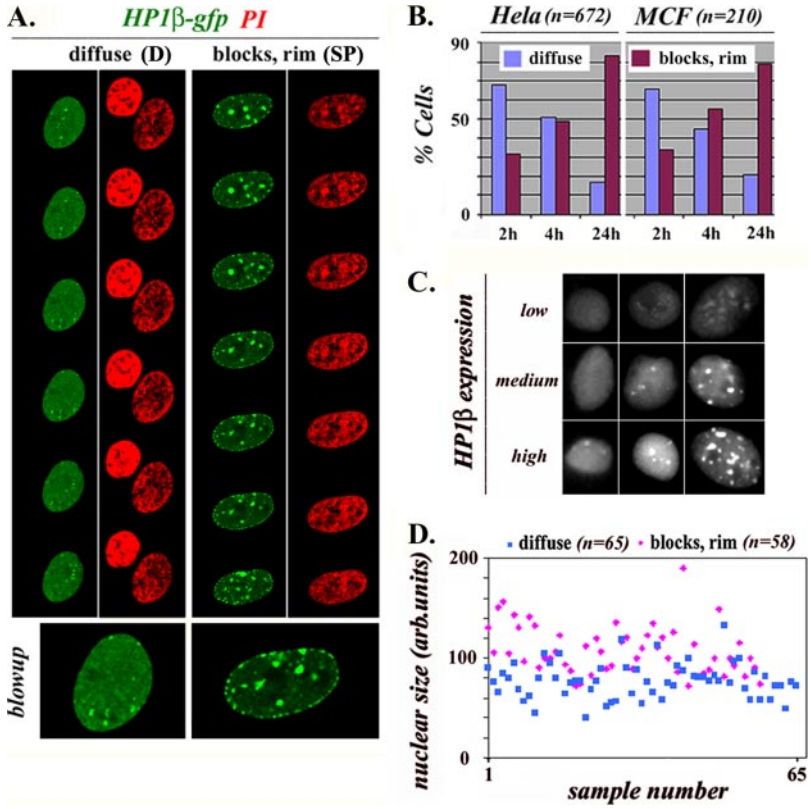

FIGURE 7. **De novo assembly of HP1 in transiently transfected human cells.** *A*, representative phenotypes after transfection of HeLa cells with HP1β-gfp and counter-staining with propidium iodide (*PI*). The columns correspond to sequential confocal sections. *B*, morphometric data from different transfection experiments, using HeLa and MCF-7 cells. The proportion of figures exhibiting diffuse or focal patterns are depicted in the histogram. *n* is the number of cells scored. *C*, relative HP1β-gfp expression levels in cells exhibiting either diffuse or focal nuclear fluorescence 6–12 h after transfection. For further explanations see "Results." *D*, relative nuclear size in transfected cells exhibiting a diffuse or a speckled phenotype. *n* is the number of cells scored. For further explanations see "Results."

mixture thereof, we obtained exclusively the D-phenotype, irrespective of plasmid uptake technique and time course (Fig. 8*D*). This was rather telling, because according to current studies (10) the CD-containing gfp-protein should have been able to target me_3K9-enriched sites.

Cell Cycle-dependent Assembly and Dynamics—As mentioned above, the nuclei of D cells were smaller than those of SP cells, suggesting cell cycle differences (nuclear size increases visibly after the G_1-phase). To explore this further, we co-injected the HP1β-gfp plasmid and the base analog Cy3-dUTP and examined the cells 6 h later. As shown in Fig. 9*A*, cells exhibiting a D pattern were in most of the cases Cy3-dUTP-negative and, therefore, non-S. When diffuse fluorescence co-existed with a Cy3-dUTP-positive staining, the distribution of the base analog was typical of an early-S cell (euchromatic replication pattern). However, in all cases where large HP1β-gfp blocks and peripheral fluorescence were detected (SP-phenotype), the cells were either Cy3-dUTP-positive (late-S, "heterochromatic" replication pattern) or early post-mitotic (*i.e.* paired, at telophase or early G_1). Cy3-dUTP and HP1β-gfp spots in late-S cells were not always coincident (Fig. 9*A*, *middle panels*), because the base analog could be apparently incorporated into replicating DNA immediately after injection, whereas the HP1β-gfp protein was synthesized with a lag.

We also monitored transfected cells that had incorporated BrdUrd (see Fig. S2 in supplemental data). In this case, the samples were examined 18 h after transfection and 30 min after incubation with this base analog. Although a smaller number of figures could be scored using this method, the results were essentially the same as with the Cy3-dUTP experiments presented above. The combined observations strongly suggested that stable incorporation of HP1β in heterochromatic domains occurs in late S-phase and at the end of mitosis. Consistent with the latter point, staining of transfected cells with anti-centromere (CREST) antibodies revealed reversible dissociation of HP1β-gfp from pericentromeric heterochromatin during cell division (Fig. 9*B*), a property shared with endogenous HP1 (45, 46).

To investigate the same problem from a different angle, we transfected cells that had been cultured either in normal medium or in the presence of cell cycle-arresting agents. As illustrated in Fig. 9*C* (*upper* panels), HP1β-gfp assembled normally in the control cells, following the usual 24-h schedule. However, when the cells were blocked at the S-phase (by either hydroxyurea, thymidine, or aphidicolin), or in G_1 (by mimosine), HP1β-gfp assembly at heterochromatic sites was inhibited and 90% of the cells exhibited a D pattern. This dramatic effect was not a consequence of "global" unbalance, because transfection of unsynchronised and cell cycle-arrested cells by control plasmids (Rab7-gfp and CD39 mutant-gfp) yielded the expected pattern in both cases (Fig. 9*C*, *middle* and *lower panels*). In line with these observations, when the cells were released from hydroxyurea block, the proportion of figures that exhibited the typical, SP pattern became increasingly higher and 8 h after entering the S-phase the majority had recruited HP1β into heterochromatin (Fig. 9, *D* and *E*). These results lead us to conclude that stable incorporation of HP1β at heterochromatic sites requires passage through the S-phase.

Recently published FRAP data on HP1-gfp transfected cells have shown that all forms of HP1-gfp exhibit rapid dynamics, with the bulk of the fluorescence returning to the bleached area within seconds (36, 45, 47, 48). To find out whether this holds in our experimental system, we performed FRAP and inverse FRAP studies on transiently transfected HeLa cells. The results (presented in Fig. S3 of supplemental data) were similar to those reported previously in refs (36, 45, 47, 48), showing rapid recovery of euchromatin-bound HP1β-gfp and slightly slower, but still very fast, kinetics of the heterochromatin-bound tracer. Consistent with the observations presented in Fig. 9, the mobility of HP1β-gfp in hudroxyurea-arrested cells was comparable with that of diffuse HP1β-gfp in non-arrested cells but much lower than the reported values of free gfp (36, 45, 47, 48), which would correspond to freely diffusible, non-bound material. From these observations we conclude that the transient

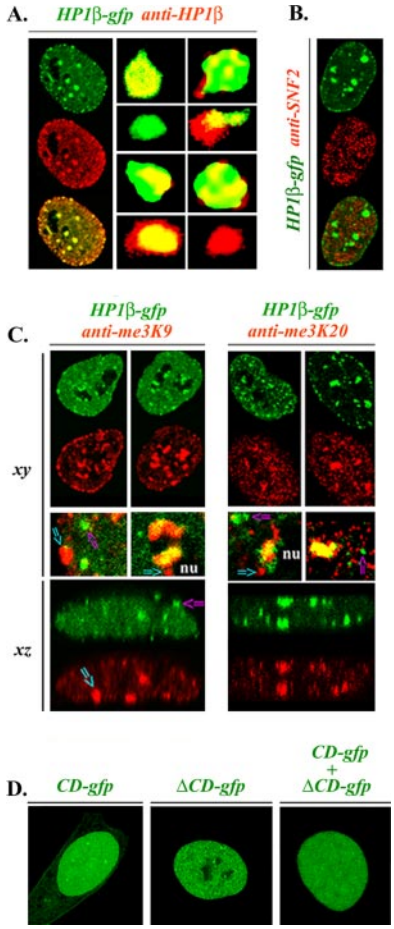

FIGURE 8. **Targeting of HP1-gfp to heterochromatic foci.** *A*, counter-staining of HP1β-gfp-transfected cells by anti-HP1β antibodies. The gallery on the *right* shows (at higher contrast and zoom) the spectrum of color patterns detected in different heterochromatic foci. For further comments see text. *B* and *C*, relative distribution of HP1β-gfp and SNF-2 (euchromatic marker) or me_3K9-H3 and me_3K20-H4 (heterochromatic markers). *xy* and *xz* sections are shown. *Arrows* indicate foci that are singly decorated (either *red* or *green*). *nu* denotes the area of the nucleolus. Other designations are as in previous figures. *D*, the same experiment as in *A*, using two HP1β deletion mutants: 1–70 (*CD-gfp*) and 69–185 (*ΔCD-gfp*).

system employed in this study does not differ significantly from the previously used models.

As puzzling as it might seem, the fact that HP1β-gfp exhibits rapid exchange, while its accumulation and stable incorporation in heterochromatic territories proceeds in a cell cycle-dependent fashion, can be rationally explained. It is possible that a subpopulation of HP1 molecules, which escapes detection by FRAP, is recruited to chromatin only when specific "windows of opportunity" arise. This small subpopulation may serve as a seed for further HP1 assembly. A speculative model based on this hypothesis and accommodating all of our *in vivo* and *in vitro* observations is presented in Fig. 10.

DISCUSSION

me_3Lys^9 as an Exclusive HP1 Binding Motif—While mis-localization of HP1 in *Suvar3,9* null cells provides compelling evidence that me_3K9-H3 is critical for HP1 targeting to heterochromatin, other interpretations are still open for discussion. Knock-out of the two *Suvar3,9* genes, apart from damping Lys^9 trimethylation, also causes a variety of downstream effects, such as abolishment of Lys^{20} trimethylation in histone H4, mis-targeting of the DNA methylase Dnmt3b and increase of Lys^{27} trimethylation in histone H3 (28, 49, 50). Thus, it is hard to distinguish whether HP1 is mis-targeted because heterochromatin architecture is globally altered or because there is a lack of appropriate binding sites.

In vitro studies bearing on the question of whether or not me_3K9 constitutes the sole binding site for HP1 sometimes yield surprising results; for instance, while H3 peptides containing me_3K9 bind HP1 with μM affinity (10, 51), oligonucleosomal arrays reconstituted from recombinant (*i.e.* unmodified) histones seem to bind with nM affinity (25). Low affinity binding of the H3 tail is consistent with the fact that synthetic peptides representing amino acids 1–15 bind weakly to HP1 but do not compete effectively with the intact protein, even at a 200-fold molar excess. This could only occur if HP1 had a higher affinity for the histone fold region of H3, as previously suggested by Nielsen and others (26, 50, 52). In line with this interpretation, we have found that HP1 binds to recombinant (*i.e.* non-modified) and trypsinized (*i.e.* tailless) H3, while HP1-selected particles of *native* heterochromatin contain a complex pattern of modifications that do not conform to the formula "me_3K9/non-acetylated K14/me_1K27" (50, 52). This is not the first time that the currently accepted histone code "rules" are violated: modification of Lys^9 (trimethylation), Ser^{10} (phosphorylation), and Lys^{14} (acetylation) have been detected recently on the *same* H3 molecule under *in vivo* conditions (53).

Multiple Pathways of HP1 Assembly—Previous work with stably transfected cells has established that at steady-state HP1α/HP1β-gfp localize in large heterochromatic blocks around nucleoli and in dense chromatin masses located at the nuclear periphery (Ref. 45 and references therein). However, when *de novo* assembly of HP1 proteins is interrogated using a transient transfection system (Ref. 36, 45, 47, 48 and this study), or microinjection of purified HP1 proteins (46), more than one phenotype is usually observed. In the latter case, accumulation of exogenous proteins in nucleoplasmic foci occurs with a considerable lag and is not completed until 24 h post-injection (*i.e.* approximately the duration of the complete cell cycle).

It is conceivable that aberrant HP1 assembly might occur as a result of physical trauma (*e.g.* injection), chemical stress (*e.g.* calcium phosphate treatment), or metabolic unbalance (*e.g.* overloading the cells with "foreign" proteins). Aware of these limitations, in this study we have examined cells that express different levels of wild type or mutant HP1 proteins, experimented with alternative transfection protocols, and tested different cellular models. Irrespective of method, we always observed two distinct HP1β-gfp patterns in human cells: in one group of cells the fluorescent protein was scattered throughout the nucleoplasm in the form of "granules," or tiny foci, whereas in another subpopulation it was fully incorporated into large blocks of heterochromatin. This phenotypic variation was not due to nuclear anomalies that can be detected by DAPI/PI and anti-histone, anti-HP1, anti-SNF-2, or anti-nuclear envelope antibody staining (Fig. 8).[6] Moreover, the relative proportions of the two phenotypes evolved in an orderly fashion upon progression of the cell cycle. These observations and the data amassed from *in vitro* studies led us to conclude that stable incorporation of HP1 proteins into peripheral and perinucleolar heterochromatin takes place only when and where nucleosome structure is altered.

The *in vivo* circumstances under which this might occur are well defined: partial or complete dissociation of the core particle could occur during transcription-associated remodeling, recombination, histone variant exchange, or even steady-state chromatin dynamics (54–56). Nevertheless, by and large, nucleosome disassembly and reassembly is known to occur during DNA replication. Supporting a replication-de-

[6] G. K. Dialynas, D. Makatsori, N. Kourmouli, P. A. Theodoropoulos, K. McLean, S. Terjung, P. B. Singh, and S. D. Georgatos, unpublished observations.

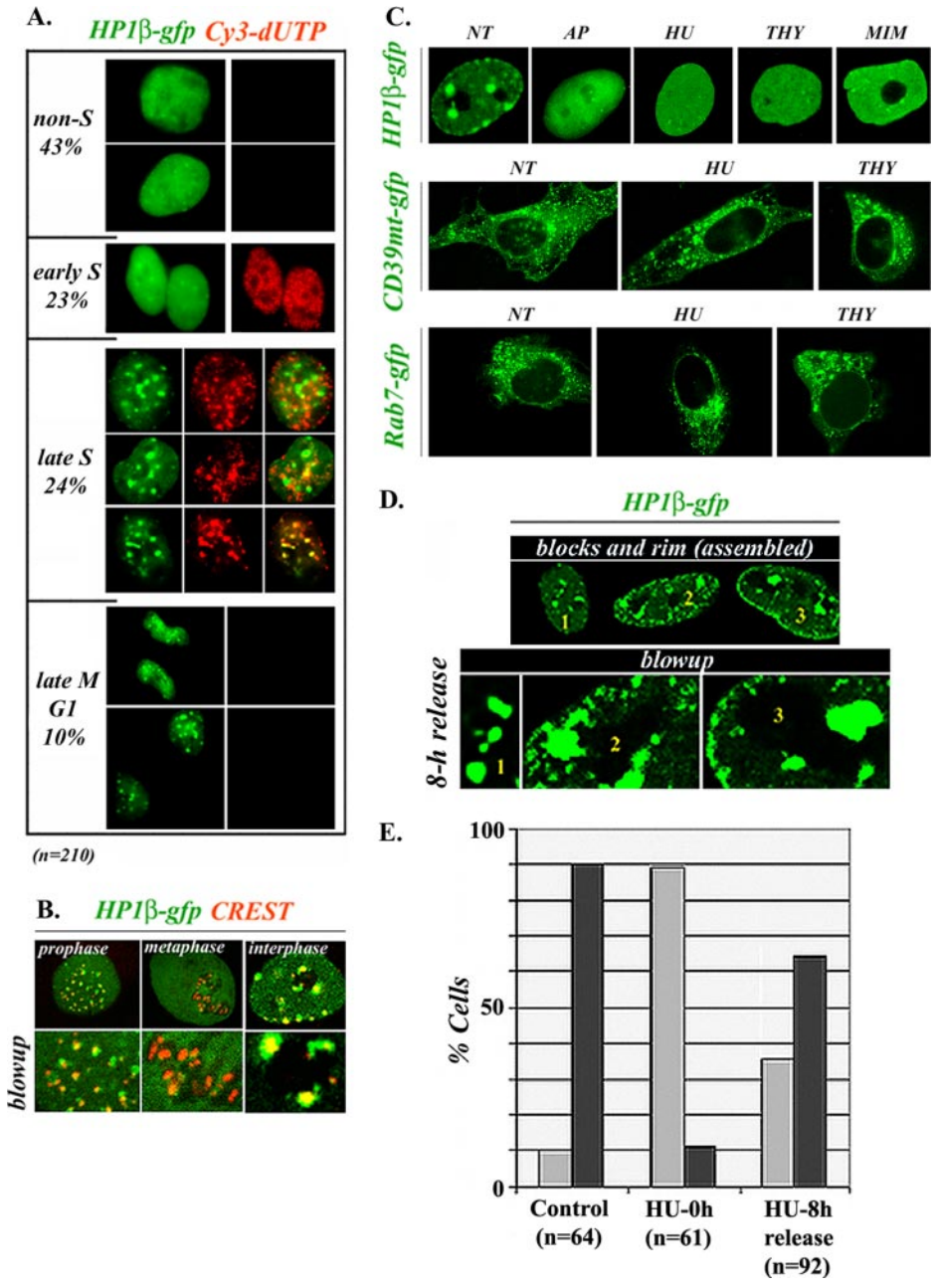

FIGURE 9. **Cell cycle dependence of HP1 assembly.** *A*, staining patterns of transfected cells 6 h after co-injection of a HP1β-gfp plasmid and Cy3-dUTP into the cytoplasm. The proportions of each phenotype are given on the *left*. *n* is the number of cells scored. *B*, relative distribution of HP1β-gfp and centromeric markers (CREST antigens) in mitotic cells. The *right-hand panel* in the blowup is rotated in comparison with the original image *C*. Distribution of HP1β-gfp, Rab7-gfp, and a CD39 mutant-gfp 24 h post-transfection in cells cultured in normal media (*NT*) or media that contained aphidicolin (*AP*), hydroxyurea (*HU*), thymidine (*THY*), or mimosine (*MIM*). *D*, resumption of HP1β-gfp assembly after release from hydroxyurea block. Representative phenotypes 8 h after transfer to normal medium are shown. The blowup shows parts of the cells that are numbered at higher contrast and zoom. *E*, morphometric data from the experiment shown in *C*. *n* is the number of cells scored. *Light gray columns*, D cells; *dark gray columns*, SP cells.

pendent pathway, labeling of transfected cells with Cy3-dUTP or BrdUrd revealed that *de novo* assembly of HP1β requires passage through the S-phase. Early after transfection, the majority (over 70%) of the cells that can recruit HP1β-gfp into peripheral and perinucleolar heterochromatin are in the late S-phase and exhibit a typical "heterochromatic/late replication" pattern. Conversely, virtually all of the cells that display diffuse HP1β-gfp fluorescence are either non-S or at the early S-phase. A diffuse pattern has never been detected in late S-phase cells, while, upon G_1 or S-phase arrest, deposition of HP1β to heterochromatic blocks is inhibited.

State and Microscopic Species of HP1—The observations reported here may appear surprising in view of FRAP studies showing rapid exchange of heterochromatin-bound HP1-gfp in mammalian and yeast cells (Refs. 36, 45, and 47 and this report). However, this discrepancy can be explained if we take into account that often the recovery of HP1-gfp is not complete, with fluorescence reaching only 70–80% of the pre-bleaching value. It is possible that heterochromatin-associated HP1 comprises several kinetically (and perhaps chemically) distinct species, one of which is highly immobile and serves a "structural" role. Opposite to loosely associated material held in place by weak interactions (36, 57), such integrated HP1 molecules would not dissociate from heterochromatin, unless the octamer structure is disrupted. Support for this idea is provided by a recent study (48) where several kinetically distinct forms of HP1 were identified. In this report, the relative amount of immobile molecules correlated with the chromatin condensation state, mounting to more than 44% in the condensed chromatin of transcriptionally silent cells.

Another interpretation, which unifies data obtained in several different laboratories, could be that steady-state dynamics and stable incorporation of HP1 proteins in human cells represent mechanistically distinct processes. Apart from nucleosome "opening", incorporation of newly synthesized HP1 into chromatin may in fact require siRNA, cell

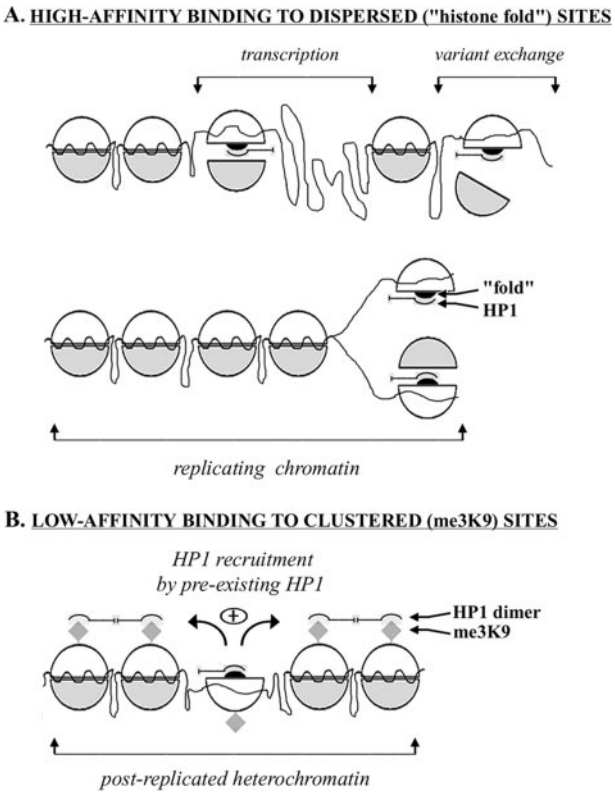

FIGURE 10. **Pathways of HP1 incorporation into chromatin.** This highly speculative model claims that assembly of HP1 proteins can proceed in two different ways. *A*, stable binding to dispersed chromatin sites (via the histone fold) that become available under specific circumstances and phases of the cell cycle. Nucleosomal DNA is represented by *wavy lines*; H2A-H2B and H3-H4 subcomplexes are shown as *shaded* or *open semicircles*, respectively. *B*, loose binding to clustered low affinity sites (through me_3K9). For more details see "Discussion."

cycle-specific modification/"licensing", or chaperoning by a specific S-phase factor.

In Fig. 10 we propose that HP1 binds initially to a variety of dispersed loci (high affinity/low capacity binding, no exchange), accessing the histone fold region of H3 that becomes exposed in regions of active transcription, histone variant exchange, or replication. Once an initial "nucleus" is assembled, HP1 may spread to non-replicating heterochromatin by binding to adjacent, clustered me_3K9 sites (low affinity/high capacity binding, rapid exchange). Obviously, if such determinants do not exist in the immediate neighborhood (*e.g.* euchromatin), only a trace amount of HP1 would remain associated with the initial sites, yielding an indistinct signal in indirect immunofluorescence assays and creating the impression of an exclusively heterochromatic localization. Our future studies are directed toward rigorously testing this working hypothesis.

Acknowledgments—Morphological work was performed at the Confocal and Video Microscopy Unit of the University of Ioannina and at Advanced Light Microscopy Facility (European Molecular Biology Laboratory). We are grateful to Anastasia Politou, Panos Kouklis, Hara Polioudaki, and Carol Murphy for intellectual contributions and materials.

REFERENCES

1. Jenuwein, T., and Allis, C. D. (2001) *Science* **293,** 1074–1080
2. Daniel, J. A., Pray-Grant, M. G., and Grant, P. A. (2005) *Cell Cycle* **4,** 919–926
3. Singh, P. B., Miller, J. R., Pearce, J., Kothary, R., Burton, R. D., Paro, R., James, T. C., and Gaunt, S. J. (1991) *Nucleic Acids Res.* **19,** 789–794
4. Brasher, S. V., Smith, B. O., Fogh, R. H., Nietlispach, D., Thiru, A., Nielsen, P. R., Broadhurst, R. W., Ball, L. J., Murzina, N. V., and Laue, E. D. (2000) *EMBO J.* **19,** 1587–1597
5. Cowieson, N. P., Partridge, J. F., Allshire, R. C., and McLaughlin, P. J. (2000) *Curr. Biol.* **10,** 517–525
6. Wang, G., Ma, A., Chow, C. M., Horsley, D., Brown, N. R., Cowell, I. G., and Singh, P. B. (2000) *Mol. Cell. Biol.* **20,** 6970–6983
7. Litt, M. D., Simpson, M., Gaszner, M., Allis, C. D., and Felsenfeld, G. (2001) *Science* **293,** 2453–2455
8. Peters, A. H., O'Carroll, D., Scherthan, H., Mechtler, K., Sauer, S., Schofer, C., Weipoltshammer, K., Pagani, M., Lachner, M., Kohlmaier, A., Opravil, S., Doyle, M., Sibilia, M., and Jenuwein, T. (2001) *Cell* **107,** 323–337
9. Schotta, G., Ebert, A., Krauss, V., Fischer, A., Hoffmann, J., Rea, S., Jenuwein, T., Dorn, R., and Reuter, G. (2002) *EMBO J.* **21,** 1121–1131
10. Jacobs, S. A., and Khorasanizadeh, S. (2002) *Science* **295,** 2080–2083
11. Bannister, A. J., Zegerman, P., Partridge, J. F., Miska, E. A., Thomas, J. O., Allshire, R. C., and Kouzarides, T. (2001) *Nature* **410,** 120–124
12. Lachner, M., O'Carroll, D., Rea, S., Mechtler, K., and Jenuwein, T. (2001) *Nature* **410,** 116–120
13. Nakayama, J., Rice, J. C., Strahl, B. D., Allis, C. D., and Grewal, S. I. (2001) *Science* **292,** 110–113
14. Ahmad, K. (2004) *Mol. Cell* **15,** 494–495
15. Cowell, I. G., Aucott, R., Mahadevaiah, S. K., Burgoyne, P. S., Huskisson, N., Bongiorni, S., Prantera, G., Fanti, L., Pimpinelli, S., Wu, R., Gilbert, D. M., Shi, W., Fundele, R., Morrison, H., Jeppesen, P., and Singh, P. B. (2002) *Chromosoma* **111,** 22–36
16. Ringrose, L., Ehret, H., and Paro, R. (2004) *Mol. Cell* **16,** 641–653
17. Greil, F., van der Kraan, I., Delrow, J., Smothers, J. F., de Wit, E., Bussemaker, H. J., van Driel, R., Henikoff, S., and van Steensel, B. (2003) *Genes Dev.* **17,** 2825–2838
18. Danzer, J. R., and Wallrath, L. L. (2004) *Development* (*Camb.*) **131,** 3571–3580
19. Vakoc, C. R., Mandat, S. A., Olenchock, B. A., and Blobel, G. A. (2005) *Mol. Cell* **19,** 381–391
20. Huang, D. W., Fanti, L., Pak, D. T., Botchan, M. R., Pimpinelli, S., and Kellum, R. (1998) *J. Cell Biol.* **142,** 307–318
21. Prasanth, S. G., Prasanth, K. V., Siddiqui, K., Spector, D. L., and Stillman, B. (2004) *EMBO J.* **23,** 2651–2663
22. Maison, C., Bailly, D., Peters, A. H., Quivy, J. P., Roche, D., Taddei, A., Lachner, M., Jenuwein, T., and Almouzni, G. (2002) *Nat. Genet.* **30,** 329–334
23. Muchardt, C., Guilleme, M., Seeler, J. S., Trouche, D., Dejean, A., and Yaniv, M. (2002) *EMBO Rep.* **3,** 975–981
24. Quivy, J. P., Roche, D., Kirschner, D., Tagami, H., Nakatani, Y., and Almouzni, G. (2004) *EMBO J.* **23,** 3516–3526
25. Fan, J. Y., Rangasamy, D., Luger, K., and Tremethick, D. J. (2004) *Mol. Cell* **16,** 655–661
26. Nielsen, A. L., Oulad-Abdelghani, M., Ortiz, J. A., Remboutsika, E., Chambon, P., and Losson, R. (2001) *Mol. Cell* **7,** 729–739
27. Perrini, B., Piacentini, L., Fanti, L., Altieri, F., Chichiarelli, S., Berloco, M., Turano, C., Ferraro, A., and Pimpinelli, S. (2004) *Mol. Cell* **15,** 467–476
28. Kourmouli, N., Jeppesen, P., Mahadevhaiah, S., Burgoyne, P., Wu, R., Gilbert, D. M., Bongiorni, S., Prantera, G., Fanti, L., Pimpinelli, S., Shi, W., Fundele, R., and Singh, P. B. (2004) *J. Cell Sci.* **117,** 2491–2501
29. Makatsori, D., Kourmouli, N., Polioudaki, H., Shultz, L. D., McLean, K., Theodoropoulos, P. A., Singh, P. B., and Georgatos, S. D. (2004) *J. Biol. Chem.* **279,** 25567–25573
30. Maison, C., Horstmann, H., and Georgatos, S. D. (1993) *J. Cell Biol.* **123,** 1491–1505
31. Bohm, L., and Crane-Robinson, C. (1984) *Biosci. Rep.* **4,** 365–386
32. Ausio, J., Dong, F., and van Holde, K. E. (1989) *J. Mol. Biol.* **206,** 451–463
33. Fletcher, T. M., and Hansen, J. C. (1995) *J. Biol. Chem.* **270,** 25359–25362
34. Chang, L., Loranger, S. S., Mizzen, C., Ernst, S. G., Allis, C. D., and Annunziato, A. T. (1997) *Biochemistry* **36,** 469–480
35. Gruss, C., Wu, J., Koller, T., and Sogo, J. M. (1993) *EMBO J.* **12,** 4533–4545
36. Cheutin, T., Gorski, S. A., May, K. M., Singh, P. B., and Misteli, T. (2004) *Mol. Cell. Biol.* **24,** 3157–3167
37. Lee, M. S., and Garrard, W. T. (1991) *EMBO J.* **10,** 607–615
38. Cartwright, I. L., and Elgin, S. C. (1986) *Mol. Cell. Biol.* **6,** 779–791
39. Yager, T. D., and van Holde, K. E. (1984) *J. Biol. Chem.* **259,** 4212–4222
40. Oohara, I., and Wada, A. (1987) *J. Mol. Biol.* **196,** 389–397
41. Oohara, I., and Wada, A. (1987) *J. Mol. Biol.* **196,** 399–411
42. Park, Y. J., Dyer, P. N., Tremethick, D. J., and Luger, K. (2004) *J. Biol. Chem.* **279,** 24274–24282
43. Luger, K., and Hansen, J. C. (2005) *Curr. Opin. Struct. Biol.* **15,** 188–196
44. Oudet, P., Germond, J. E., Sures, M., Gallwitz, D., Bellard, M., and Chambon, P. (1978) *Cold Spring Harb. Symp. Quant. Biol.* **42,** 287–300
45. Cheutin, T., McNairn, A. J., Jenuwein, T., Gilbert, D. M., Singh, P. B., and Misteli, T. (2003) *Science* **299,** 721–725
46. Kourmouli, N., Theodoropoulos, P. A., Dialynas, G., Bakou, A., Politou, A. S., Cowell, I. G., Singh, P. B., and Georgatos, S. D. (2000) *EMBO J.* **19,** 6558–6568
47. Festenstein, R., Pagakis, S. N., Hiragami, K., Lyon, D., Verreault, A., Sekkali, B., and

Kioussis, D. (2003) *Science* **299,** 719–721
48. Schmiedeberg, L., Weisshart, K., Diekmann, S., Meyer Zu Hoerste, G., and Hemmerich, P. (2004) *Mol. Biol. Cell* **15,** 2819–2833
49. Lehnertz, B., Ueda, Y., Derijck, A. A., Braunschweig, U., Perez-Burgos, L., Kubicek, S., Chen, T., Li, E., Jenuwein, T., and Peters, A. H. (2003) *Curr. Biol.* **13,** 1192–1200
50. Schotta, G., Lachner, M., Sarma, K., Ebert, A., Sengupta, R., Reuter, G., Reinberg, D., and Jenuwein, T. (2004) *Genes Dev.* **18,** 1251–1262
51. Jacobs, S. A., Taverna, S. D., Zhang, Y., Briggs, S. D., Li, J., Eissenberg, J. C., Allis, C. D., and Khorasanizadeh, S. (2001) *EMBO J.* **20,** 5232–5241
52. Fischle, W., Wang, Y., and Allis, C. D. (2003) *Nature* **425,** 475–479
53. Mateescu, B., England, P., Halgand, F., Yaniv, M., and Muchardt, C. (2004) *EMBO Rep.* **5,** 490–496
54. Flaus, A., and Owen-Hughes, T. (2004) *Curr. Opin. Genet. Dev.* **14,** 165–173
55. Korber, P., and Horz, W. (2004) *J. Biol. Chem.* **279,** 35113–35120
56. Kimura, H., and Cook, P. R. (2001) *J. Cell Biol.* **153,** 1341–1353
57. Singh, P. B., and Georgatos, S. D. (2002) *J. Struct. Biol.* **140,** 10–16